

THE TRANSPORT PROPERTIES OF CO₂ AND CH₄ FOR TRIMETHYLSILYLATED POLYSULFONE MEMBRANE

Hyun-Joon Kim and Suk-In Hong[†]

Department of Chemical Engineering, Korea University, 1, 5-ka, Anam-dong, Sungbuk-ku, Seoul 136-701, Korea
(Received 19 May 1997 • accepted 10 July 1997)

Abstract – The transport properties of CO₂ and CH₄ for TMSPSf (bisphenol A trimethylsilylated polysulfone) were measured, and compared with the values for PSf (bisphenol A polysulfone) and MPSf (bisphenol A methylated polysulfone) to explain the effect of molecular structure of polysulfones on gas transport properties. The permeability coefficients of three polysulfones rank in the order: TMSPSf > PSf > MPSf. TMSPSf is several times more permeable than PSf. The effect of the substituents on chain packing was related to the gas transport properties. The ranking of permeability coefficient correlates well with fractional free volume. The variation of d-spacing is also reasonably consistent with the permeability coefficient. The effects of pressure on the sorption and permeation properties of polysulfones were examined. The permeation properties for a mixture of CO₂ and CH₄ were also measured and these results were compared with the values of pure gases. The sorbed concentrations and permeability coefficients are well fitted to dual mode model. The permeability coefficients of each gas of binary mixture are reduced than those for pure gases, and the extent of reduction in permeability coefficient is the smallest for TMSPSf, which has the highest value of Langmuir capacity constant.

Key words: Trimethylsilylated Polysulfone, Sorption, Permeation, Mixed Gas

INTRODUCTION

Membrane-based gas separation technology has emerged as an important alternative technology to cryogenic distillation or pressure swing adsorption. New materials with higher permeability and selectivity are required to advance membrane technology in the commercial areas. It is generally known that polymeric membrane which has high gas permeability exhibits low selectivity and *vice versa* [Stern, 1994; Koros and Fleming, 1993]. Careful molecular design of polymer structure can lead to materials that can run counter to a certain extent this trade-off relationship. Recent studies have been focused at systematically varying polymer structure to increase permeability with minimum selectivity losses [McHattie et al., 1991a; Muruganandam et al., 1987; Ghosal et al., 1996; Pixton and Paul, 1995; Ghosal et al., 1995]. Structural changes that inhibit chain packing can increase permeability and those that reduce chain mobility can lead to higher selectivity [Kim et al., 1988; Aitken et al., 1992].

Bisphenol A polysulfone (PSf) has been used commercially as a gas separation membrane material, and it has a stable aromatic backbone that is amenable to structural modification.

Recently, some polymer materials containing silicon on the polymer branches such as poly(trimethylsilylmethyl methacrylate), poly(vinyl trimethylsilane) and poly(trimethylsilyl propyne) are well recognized to be promising membrane materials [Muller 1991; Ichiraku et al., 1987]. These materials have exceptionally high permeabilities, but the disadvantage of these polymers is their low selectivities. Considering this fact, this present work

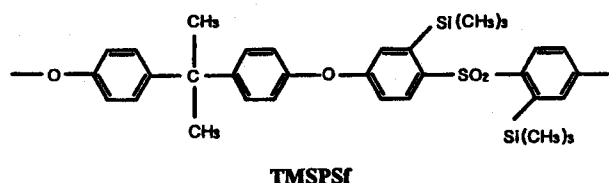
involves the synthesis of bisphenol A trimethylsilylated polysulfone (TMSPSf). The gas pair chosen for this study is the CO₂/CH₄ system. The separation of these gases is of interest in oil recovery, the treatment of landfill gases and sweetening of natural gases [Bhide and Stern, 1987; Bollinger et al., 1982; Rautenbach and Welsch, 1994]. In this study, the transport properties of CO₂ and CH₄ for TMSPSf were measured, and compared with the values for PSf and MPSf (bisphenol A methylated polysulfone), which have been studied previously in our laboratory [Kim and Hong, 1997], to explain the effect of molecular structure of polysulfones on gas transport properties. In addition, the effects of feed pressure on the transport properties were examined. The permeation properties for a mixture of CO₂ and CH₄ are also measured, and these results are compared with those for pure gases.

EXPERIMENTAL

1. Materials

Bisphenol A polysulfone (PSf, Udel® P-3500) was obtained from Amoco Chemical Co.. Reagent grade tetrahydrofuran (THF) was freshly distilled for each reaction. All other reagents were purchased commercially and used as received without further purification. The procedure described by Guiver et al. [1989a, 1989b] was used for the synthesis of TMSPSf. PSf (0.027 mol, 12 g) was dissolved in distilled THF (400 mL) and the temperature of the solution was reduced to below -30 °C. n-Butyllithium (0.06 mol, 6 mL of 10 M in hexane) was added dropwise. The mixture turned a red-brown color. The polymer was trimethylsilylated after 30 min by the dropwise

[†]To whom all correspondence should be addressed.



TMSPSf

Fig. 1. Chemical structures of TMSPSf.

addition of excess trimethylsilyl chloride. The resulting solution was stirred for 1 hr, and then precipitated into methanol, washed several times, and finally dried to yield TMSPSf. The chemical structure of TMSPSf was characterized by ¹H-NMR and ¹³C-NMR, and are shown in Fig. 1. The degree of substitution (DS) was calculated by comparative methyl integration of the substituent and the isopropylidene group. The DS was over 70 %.

2. Characterization

¹H-NMR and ¹³C-NMR spectra were recorded on a Bruker DRX-500 sepectrophotometer. The glass transition temperature (*T_g*) for each material was measured using a Perkin-Elmer DSC-7 differential scanning calorimeter at a heating rate of 20 °C/min. Polymer density was measured using a density gradient column filled with aqueous solutions of calcium nitrate at 23 °C. Fractional free volume of the polymers was calculated by the group contribution method proposed by Bondi [Bondi, 1964; Van Krevelen, 1990]. The wide-angle X-ray diffraction (WAXD) measurements were carried out using Rigaku WAXD-D/Max III B X-ray diffractometer with Cu K α radiation with wavelength of 1.54 Å. The average intersegmental distances or "d-spacings" were calculated from Bragg equation [Balta-Calleja and Vonk, 1989], $n\lambda = 2d \sin \theta$, at the angle of maximum peak of scan. Cohesive energy density (CED) was estimated by the group contributions published by Fedor [Van Krevelen, 1990].

3. Membrane Preparation

The membranes were cast from 10 wt% solution in chloroform on the clean glass plate at room temperature. The membranes were dried under atmosphere for 24 hr, controlling the rate of solvent removal. After drying, the membranes were lifted from the glass plate, and completely dried in a vacuum oven at 150 °C for several days.

4. Gas Sorption and Permeation

Pure gas sorption measurements were made for CO₂ and CH₄ up to 25 atm and at 30 °C. Equilibrium sorption was measured in the two-volume pressure decay type of sorption cell [Kim and Hong, 1997].

Permeability measurements were also made for pure CO₂ and CH₄ and their binary mixture using the variable volume method employed in our laboratory [Hong et al., 1996]. The volumetric flow rate through the membrane to the downstream side was determined by observing the displacement of 1-propanol in the capillary tube connected to the downstream side. The permeability coefficients were calculated by Eq. (1) and (2). Permeation runs were carried out at 30 °C and pressures up to 25 atm.

$$P = \bar{D} \cdot \bar{S} = \frac{J_s L}{P_1 - P_2} \quad (1)$$

$$J_s = \frac{\pi d^2}{4A} \frac{273.15 p_b}{76T} \frac{dh}{dt} \quad (2)$$

where, *P* [Barrer, cm³(STP)cm/cm²s cmHg] is the mean permeability coefficient, *D* [cm²/s] is the apparent diffusion coefficient, and *S* [cm³(STP)/cm³ cmHg] is the apparent solubility coefficient. *J_s* [cm³(STP)/cm²s] is the steady-state rate of gas permeation through unit area when the constant gas pressure *p₁* and *p₂* are maintained at the membrane interface, and *L* [cm] is the effective membrane thickness. *d* [cm] is the diameter of capillary, *A* [cm²] is the membrane permeation area, *p_b* [cmHg] is the barometric pressure, *T* [K] is the experimental temperature, and *dh/dt* is the displacement rate of propanol in the capillary. The permeation rates for the components of binary gas mixture of CO₂ and CH₄ (CO₂/CH₄=57.5/42.5 vol %) were determined by the volumetric flow rate of gas mixture and the concentration of each component on the upstream and downstream side. The concentrations of the components were determined by Gas Chromatograph (Shimatzu 8A) with a column packed with Porapak Q. Permeation runs for the binary mixture were carried out at stage cuts below 0.01.

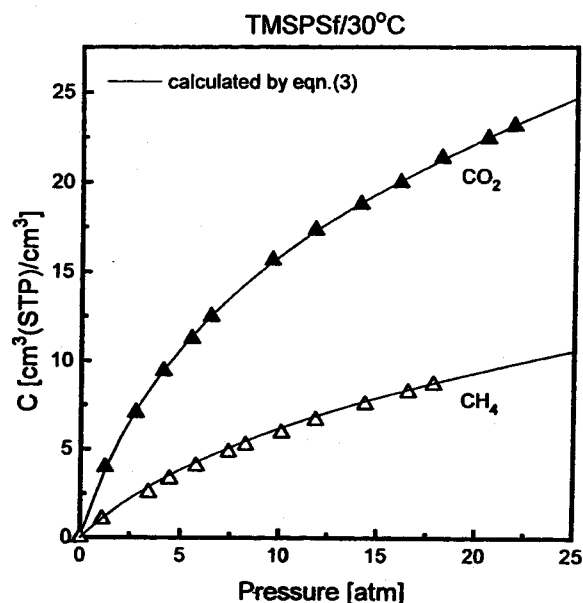
RESULTS AND DISCUSSION

1. Pure Gas Sorption and Permeation-Dual Mode Model

Sorption isotherms for CO₂ and CH₄ in TMSPSf are shown in Fig. 2 and 3. The pure gas sorption isotherms show concave to the pressure axis, and can be described by "dual sorption model" [Vieth et al., 1966]. According to dual sorption model, the equilibrium concentration of sorbed gas in glassy polymers can be described as a function of pressure:

$$C = C_D + C_H$$

$$C = k_D p + \frac{C_H b p}{1 + b p} \quad (3)$$

Fig. 2. Sorption isotherms for CO₂ and CH₄ in TMSPSf at 30 °C.

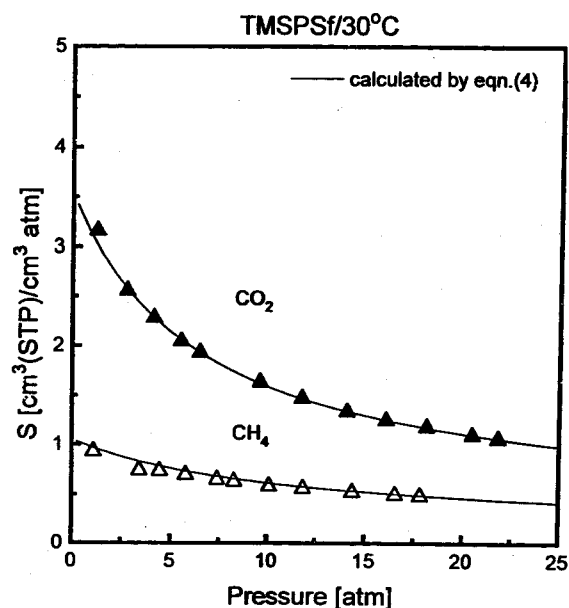


Fig. 3. Pressure dependency of solubility coefficients of CO₂ and CH₄ in TMSPSf at 30 °C.

where C [cm³(STP)/cm³] is the equilibrium concentration of the sorbed gas, and C_D and C_H represent Henry's law mode sorption and Langmuir mode sorption, respectively. The parameter k_D [cm³(STP)/cm³ atm] is the Henry's law solubility constant, C_H [cm³(STP)/cm³] is the Langmuir capacity constant, and b [atm⁻¹] is the Langmuir affinity constant. These sorption parameters can be obtained by nonlinear least-square regression, and are listed Table 1. The solid curves in Fig. 2 represent the dual mode fits of the actual data, substituting the values of sorption parameters given in Table 1. It is shown that the sorption of pure CO₂ and CH₄ in TMSPSf are well fitted by dual sorption model. Fig. 3 represents the corresponding plot of apparent solubility coefficient versus gas pressure. The apparent gas solubility coefficients in glassy polymers are decreasing function of pressure as illustrated by Eq. (4), and equal to the secant slope of the sorption isotherms.

$$\bar{S} \equiv \frac{C}{p} = k_D + \frac{C_H b}{1 + bp} \quad (4)$$

In Fig. 3, the apparent solubility coefficients decrease as the Langmuir sorption sites are saturated, and approaches the as-

Table 1. Dual mode parameters^a for TMSPSf, PSf^b, and MPSf^b at 30 °C

Polymer	Gas	k_D	C_H	b	D_D	D_H
TMSPSf	CO ₂	0.324	20.72	0.155	30.97	1.202
	CH ₄	0.199	8.30	0.090	3.521	0.221
PSf ^b	CO ₂	0.630	16.50	0.356	4.799	0.581
	CH ₄	0.167	9.04	0.118	0.692	0.106
MPSf ^b	CO ₂	0.482	12.17	0.287	2.846	0.452
	CH ₄	0.078	7.35	0.108	0.520	0.051

^aUnits: k_D [cm³(STP)/cm³ atm]; C_H [cm³(STP)/cm³]; b (atm⁻¹); $D_D \times 10$ (cm²/s); $D_H \times 10$ (cm²/s)

^bData from Kim, H. J. and Hong, S. I., 1997.

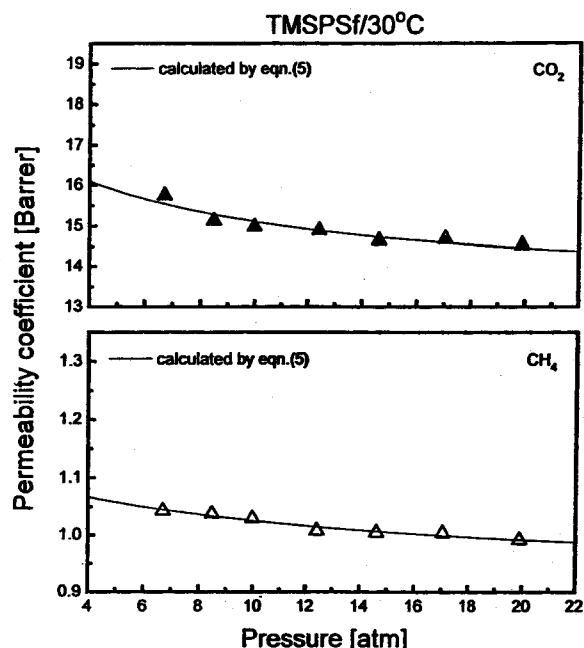


Fig. 4. Pressure dependency of permeability coefficients of CO₂ and CH₄ for TMSPSf at 30 °C.

ymptotic value of Henry's law solubility constant, k_D . The degree of pressure dependency of solubility coefficients varies with gases. The greater pressure-dependency of CO₂ solubility coefficient is due to the larger value of C_H for CO₂ compared with that for CH₄.

The permeability coefficients of pure gases for TMSPSf are shown as a function of upstream pressure in Fig. 4. The permeability coefficients of CO₂ and CH₄ decrease with increasing upstream pressure, as is often the case with other glassy polymers [Koros and Chern, 1987]. This pressure-dependency of permeability coefficients have been generally described as "dual mobility model" (or "partial immobilization model") proposed by Paul and Koros [1976]. According to dual mobility model, the populations in each the sorptions can be assigned separate diffusion coefficients D_D and D_H , the permeability coefficient of pure gas can be written as;

$$P = k_D D_D \left[1 + \frac{FK}{(1 + bp_1)(1 + bp_2)} \right] \quad (5)$$

where, $K = \frac{C_H b}{k_D}$ and $F = \frac{D_H}{D_D}$

The diffusion coefficients, D_D and D_H are calculated from the slope and intercept of the plot of experimental permeability coefficient versus $1/(1+bp_1)(1+bp_2)$. The diffusion coefficients obtained by this analysis are also listed in Table 1. The solid curves in Fig. 4 are calculated by Eq. (5) using parameters given in Table 1, and show that the permeability coefficients of CO₂ and CH₄ for TMSPSf are well fitted to dual mobility model at entire pressure range.

2. The Effect of Substituents on Permeation Properties

The comparisons of the permeability coefficients of CO₂ and CH₄ and ideal separation factors for PSf, MPSf, and TMSPSf

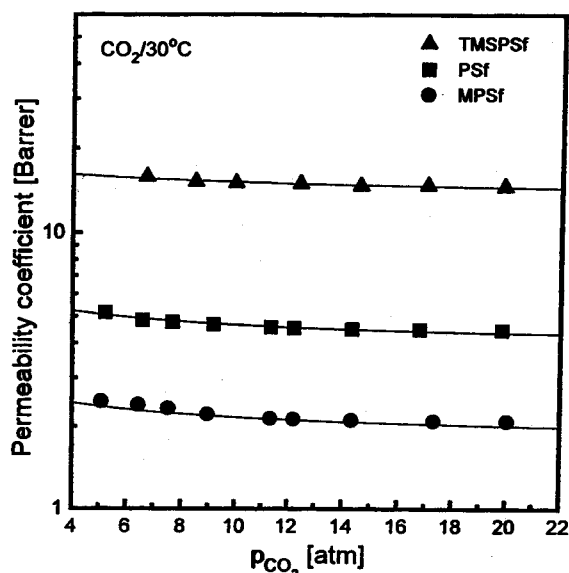


Fig. 5. Permeability coefficients of CO₂ for TMSPSf, PSf, and MPSf at 30 °C.

are shown in Figs. 5-7, and these values at 10 atm are listed in Table 2. Ideal separation factor was calculated from the ratio of the pure component permeability coefficients, i.e. P_{CO_2}/P_{CH_4} . In Figs. 5-7 and Table 2, the data for PSf and MPSf (methylated polysulfone), which have been studied previously in our laboratory [Kim and Hong, 1997], are also included to compare with TMSPSf. MPSf is the polymer in which ortho sites of sulfone unit in PSf have been replaced with methyl groups. In this study, the permeability coefficients of three polysulfones rank for CO₂ and CH₄ in the following order, TMSPSf>PSf>MPSf, and ideal separation factors are in the opposite order. The ideal separation factor for TMSPSf is reduced by about 25 % than that for PSf, but TMSPSf is several times more permeable than PSf. This result means that

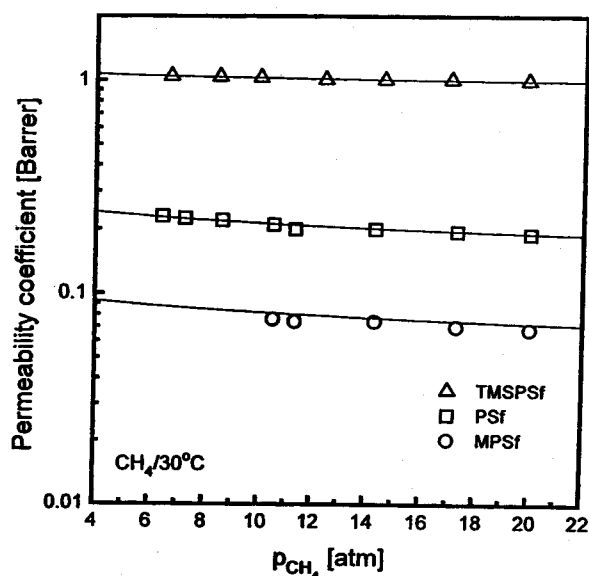


Fig. 6. Permeability coefficients of CH₄ for TMSPSf, PSf, and MPSf at 30 °C.

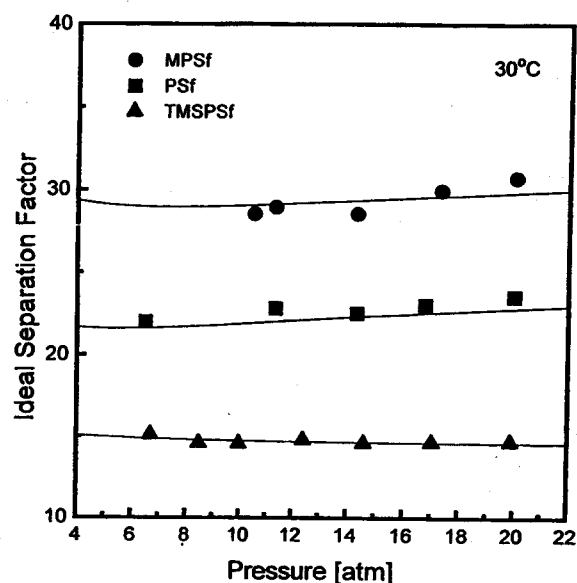


Fig. 7. Ideal separation factors of CO₂ and CH₄ for TMSPSf, PSf, and MPSf at 30 °C.

TMSPSf is strong candidate for CO₂/CH₄ separation membrane.

In general, the permeation properties depend on intermolecular packing distance, chain stiffness, polymer-polymer interaction and polymer-penetrant interaction. The physical properties related to permeation properties are listed in Table 3. Intermolecular packing distance is determined from fractional free volume (FFV) or d-spacing. The FFV, given in Table 3, is calculated Eq. (6). The group contribution method of Bondi [Van Krevelen, 1990] is used to calculate V_o , hypothetical specific volume of the polymer at 0 K, and V , specific volume of the polymer at T, is determined from the polymer density.

$$FFV = \frac{V - V_o}{V} \quad (6)$$

As shown in Table 2 and 3, the ranking of permeability coefficient correlates well with FFV. Fig. 8 represents the correlation of permeability coefficients with $1/FFV$ for CO₂

Table 2. Transport properties^a of CO₂ and CH₄ for TMSPSf, PSf^b, and MPSf^b at 30 °C and 10 atm

Polymer	P_{CO_2}	α_{CO_2/CH_4}	S_{CO_2}	S_{CO_2/CH_4}	D_{CO_2}	D_{CO_2/CH_4}
TMSPSf	15.1	16	2.1	2.7	7.2	5.5
PSf ^b	4.6	22	2.4	2.8	1.9	7.8
MPSf ^b	2.2	29	1.8	3.0	1.2	9.6

^aUnits: $P \times 10^{10}$ [cm³(STP) cm/s cm² cmHg]; $D \times 10^8$ (cm²/s); $S \times 10^2$ [cm³ (STP)/cm³ cmHg]

^bData from Kim, H. J. and Hong, S. I., 1997.

Table 3. Physical properties for TMSPSf, PSf^a, and MPSf^a

Polymer	T_g (°C)	ρ (g/cm ³)	d-spacing (Å)	δ (cal/cm ³) ^{1/2}	FFV
TMSPSf	164.0	1.126	5.6	11.0	0.167
PSf ^a	190.3	1.243	5.2	12.4	0.158
MPSf ^a	177.6	1.213	5.2	12.1	0.151

^aData from Kim, H. J. and Hong, S. I., 1997.

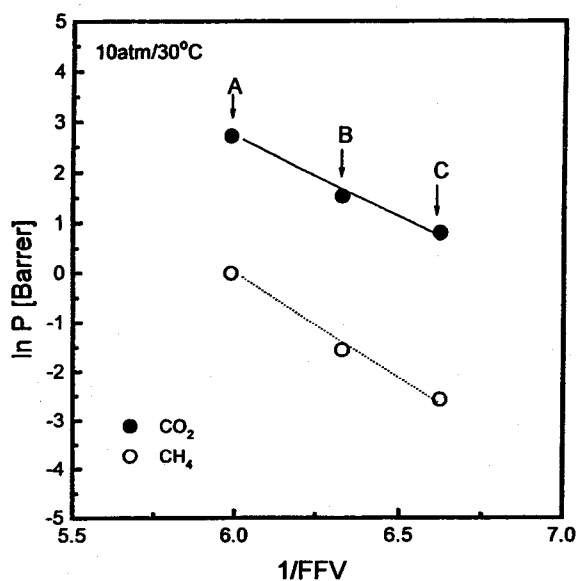


Fig. 8. Correlation of permeability coefficients at 10 atm and 30 °C with inverse fractional free volume; A=TMSPSF, B=PSf, and C=MPSf.

and CH_4 . The substitutions of bulky trimethylsilyl groups are responsible for the higher FFV of TMSPSF. The variation of d-spacing is also reasonably consistent with the permeability coefficient, although Jacobson [1991] suggested that d-spacing may not always be sensitive to intermolecular packing. For example, TMSPSF has the highest d-spacing of 5.6 Å, and the highest permeability coefficient of 15.1 Barrer at 10 atm. MPSf has lower value of FFV with the similar value of d-spacing in spite of the substitution of phenyl hydrogens of PSf with methyl groups. This result discussed in previous paper in detail [Kim and Hong, 1997].

It is generally known that the glass transition temperature is a pragmatic measure of the chain stiffness of polymer backbone, and chain stiffening leads to high permselectivity [McHattie, 1991c; McHattie, 1992]. For glassy polymers, no direct correlation is apparent between T_g and polymer gas transport properties [McHattie et al., 1991b; McHattie et al., 1991c; McHattie et al., 1992]. In our study, however, the value of T_g TMSPSF is more than 20 °C lower than that of PSf. The lower ideal separation factors of TMSPSF may be attributed, at least in part, to the lower T_g of these polymers. Cohesive energy density (CED) is also an important factor for prediction of structure-permselectivity relationships. The higher the CED, the higher the attractive forces between polymer chains. Cohesive energy density is usually expressed in terms of solubility parameter δ [$(\text{cal}/\text{cm}^3)^{1/2}$], where $\delta = (\text{CED})^{1/2}$, and the values of solubility parameter are listed in Table 3. The lower ideal separation factor of TMSPSF is due to decreasing of interchain interaction as substitution of very bulky trimethylsilyl groups.

The diffusivity and solubility contributions to both permeability and ideal separation factor of each polymer are also shown in Table 2. For each polymer diffusivity effect are larger. For example, for CO_2 , TMSPSF is 3.3 times more permeable than PSf. The CO_2 solubility coefficient of TMSPSF is

25 % lower than that of PSf, while the CO_2 diffusivity coefficient of TMSPSF is almost four times that of PSf. The ideal separation factor is the product of diffusivity selectivity and solubility selectivity. In this study, the diffusivity selectivity difference among the polymers is more significant than the solubility selectivity difference. Therefore, the variation of ideal separation factor among three polysulfones is mainly depend on the differences in diffusivity selectivity.

3. Mixed Gas Permeation

The permeability coefficients for CO_2 of binary mixture ($\text{CO}_2/\text{CH}_4=57.5/42.5$ vol%) through TMSPSF membranes are illustrated in Fig. 9, and those for CH_4 are shown in Fig. 10. In Fig. 9 and 10, the data for PSf and MPSf are also included for comparison. The solid curves in Fig. 9 and 10 represent the values calculated from pure gas data by Eq. (5) based on the respective partial pressures, and which is to compare mixed gas permeabilities with the values of pure gases at the same partial pressure. For each polymer, mixed gas permeability coefficients are lower than the respective pure component values. Such a reduction in permeability coefficient in binary mixture is commonly observed in other polymers [Ghosal et al., 1996; Chern et al., 1984]. In this study, the extent of depression in permeability coefficient is larger for less permeable polymer. For example, at 10 atm, the CO_2 mixed permeability coefficient for TMSPSF is decreased by about 2 %, but the values for MPSf is decreased by 20 % relative to the permeability coefficient of pure CO_2 .

Based on dual mode model for pure gas, Story and Koros [1989] extended the model to the case of gas mixtures in glassy polymers. For cases involving only weak penetrant-penetrant and penetrant-polymer interactions, Story and Koros [1989] assumed that the primary effect for a mixture is competition by the various penetrants for the fixed unrelaxed volume in the polymer, and that diffusivity of a penetrant in the polymer is not much changed by introducing a second com-

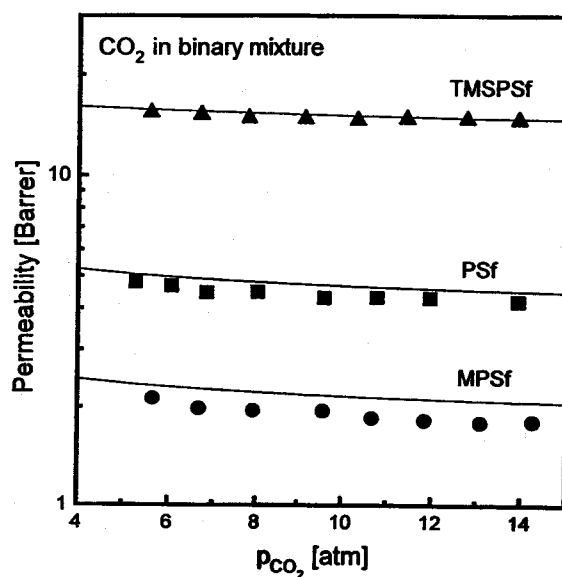


Fig. 9. Permeability coefficients for CO_2 in CO_2/CH_4 mixture (57.5/42.5 vol%) through TMSPSF, PSf, and MPSf at 30 °C. The solid lines represent calculated values by Eq. (5).

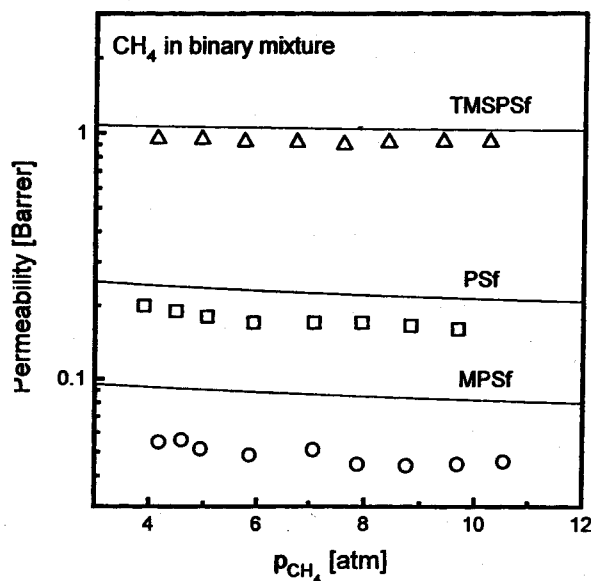


Fig. 10. Permeability coefficients for CH₄ in CO₂/CH₄ mixture (57.5/42.5 vol%) through TMSPSf, PSf, and MPSf and 30 °C. The solid lines represent calculated values by Eq. (5).

ponent.

For component A in binary mixture, the concentration of sorbed gas can be written as Eq. (7).

$$C_A = k_{DA} P_A + \frac{C_{HA} b_A P_A}{1 + b_A P_A + b_B P_B} \quad (7)$$

where subscripts A and B represent components A and B, and all the parameters are obtained by pure gas experiment. According to above assumption and Eq. (7), the permeability depressions in Fig. 9 and 10 due to the solubility effect, and result from the competition between CO₂ and CH₄ for the Langmuir sites in glassy polymers. When A and B are relatively noninteracting components, component B fills some of the Langmuir sites previously available to A in the absence of B. The lowering of the concentration driving force of A lowers its flux through the membrane. Therefore the permeability of A in binary mixture is lower than that of pure A [Kesting and Fritzsche, 1993]. In Fig. 9 and 10, the permeability depressions are the smallest for TMSPSf. This result is attributed to larger value of C_H for TMSPSf. For each polymer, the depression is larger for CO₂. This can be explained by the fact that the value of b for CO₂ is higher than for CH₄, so the depression of permeability coefficient of CH₄ in a binary mixture is higher than that of CO₂, as expected by Eq. (7).

The separation factor, α is defined as Eq. (8)

$$\alpha_{(A/B)} = \frac{y_A/y_B}{x_A/x_B} \quad (8)$$

where y 's and x 's are the mole fraction of the components in the downstream and upstream, respectively. When the pressure of the downstream is very small compared with the upstream pressure, the separation factor will be approximately equal to the ratio of permeabilities, P_A/P_B . Fig. 11 represents

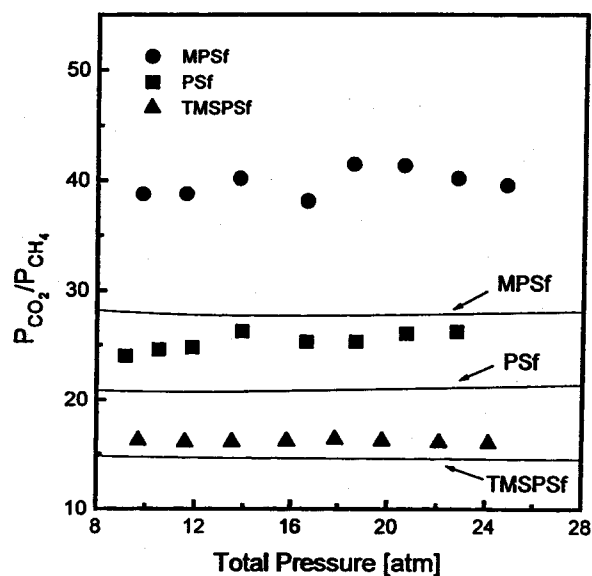


Fig. 11. Separation factors for CO₂ and CH₄ in CO₂/CH₄ mixture (57.5/42.5 vol%) through TMSPSf, PSf, and MPSf at 30 °C. The solid lines represent calculated values from the ratio of pure gas permeability coefficients without considering competition effect.

the separation factors obtained by the ratio of mixed gas permeabilities. The solid lines in Fig. 11 correspond to calculated values by Eq. (5), without considering the competition effect. The mixed gas permselectivity is higher than the pure gas value, which also shows the competition effect between each component. As explained above, the depression of permeability coefficient of CH₄ in binary gas mixture is higher than that of CO₂, so the separation factor of mixed gas is higher than the value without considering competition effect.

CONCLUSIONS

Bisphenol A trimethylsilylated polysulfone (TMSPSf) is synthesized. The substitutions of very bulky trimethylsilyl groups show the strong effect on chain packing and stiffness. The replacement of phenylene hydrogens of PSf with trimethylsilyl groups results in decreases in chain stiffness and increases in both fractional free volume and WAXD d-spacing. TMSPSf is more than three times permeable than PSf. The higher value of permeability coefficient for TMSPSf is due to higher chain packing distance.

For each polymer, the permeability coefficients for each gas of binary mixture (CO₂/CH₄=57.5/42.5 vol%) are lower than the respective values of pure gases. The extent of such a depression is the smallest for TMSPSf. The sorption and permeation of CO₂ and CH₄ for TMSPSf in this study are well described by dual-mode model. The difference among polysulfones in permeability and separation factor is mainly depend on the differences in diffusivity and diffusivity selectivity.

NOMENCLATURE

A : permeation area [cm²]

- b : Langmuir affinity constant [cmHg^{-1}]
 C : sorbed concentration [$\text{cm}^3(\text{STP})/\text{cm}^3$]
 C_H : Langmuir capacity constant [$\text{cm}^3(\text{STP})/\text{cm}^3$]
 D : diffusion coefficient [cm^2/sec]
 d : diameter of capillary tube [cm]
 h : height of capillary tube [cm]
 J : diffusion flux [$\text{cm}^3(\text{STP})/\text{cm}^2 \text{ sec}$]
 k_D : Henry's law solubility constant [$\text{cm}^3(\text{STP})/\text{cm}^3 \text{ cmHg}$]
 L : membrane thickness [cm]
 P : permeability coefficient [$\text{cm}^3(\text{STP}) \text{ cm}/\text{cm}^2 \text{ sec cmHg}$]
 p : pressure [cmHg^{-1}]
 S : solubility coefficient [$\text{cm}^3(\text{STP})/\text{cm}^3 \text{ cmHg}$]
 T : temperature [K]
 t : time [sec]
 x : mole fraction of upstream of the membrane
 y : mole fraction of downstream of the membrane

Greek Letters

- α : separation factor
 Δ : solubility parameter

Subscripts

- A : component A
 B : component B
 D : Henry's law mode
 H : Langmuir mode
 S : steady state
 1 : upstream of the membrane
 2 : downstream of the membrane

REFERENCES

- Aitken, C. L., Koros, W. J. and Paul, D. R., "Effect of Structural Symmetry on Gas Transport Properties of Polysulfones", *Macromolecules*, **25**, 3424 (1992).
 Balta-Calleja, F. J. and Vonk, C. G., "The Theory of Coherent X-Ray Scattering", in "X-Ray Scattering of Synthetic Polymers", Elsevier, Amsterdam, The Netherlands, 1 (1989).
 Bhide, B. D. and Stern, S. A., "Membrane Processes for the Removal of Acid Gases from Natural Gas. I. Process Configurations and Optimization of Operating Conditions", *J. Membrane Sci.*, **81**, 209 (1993).
 Bollinger, W. A., MacLean, D. S. and Narayan, R. S., "Separation Systems for Oil Refining and Production", *Chem. Eng. Prog.*, **Oct.**, 27 (1982).
 Bondi, A., "Van der Waals Volume and Radii", *J. Phys. Chem.*, **68**, 441 (1964).
 Chern, R. T., Koros, W. J., Yuri, B., Hopenberg, H. B. and Stanett, V. T., "Selective Permeation of CO_2 and CH_4 through Kapton Polyimide; Effects of Penetrant Competition and Gas Phase Nonideality", *J. Polym. Sci., Part B, Polym. Phys. Ed.*, **22**, 1061 (1984).
 Ghosal, K., Freeman, B. D., Chern, R. T., Alvarez, J. C., de la Campa, J. G., Lozano, A. E. and de Abajo, J., "Gas Separation Properties of Aromatic Polyamides with Sulfone Groups", *Polymer*, **36**, 793 (1995).
 Ghosal, K., Chern, R. T., Freeman, B. D., Daly, W. H. and Negulescu, I. I., "Effect of Basic Substituents on Gas Sorption and Permeation in Polysulfones", *Macromolecules*, **29**, 4360 (1996).
 Guiver, M. D., Kutowy, O. and ApSimon, J. W., "Functional Group Polysulphones by Bromination-Metalation", *Polymer*, **30**, 1137 (1989a).
 Guiver, M. D., ApSimon, J. W. and Kutowy, O., "Preparation of Substituted Polysulfones through Ortho-Metalated Intermediates", U. S. Patent 4,797,457 (1989b).
 Hong, S. I., Kim, H. J., Park, H. Y., Kim, T. J. and Jeong, Y. S., "Study of Polysulfone Membrane for Membrane-Covered Oxygen Probe System", *J. of Korean Ind. & Eng. Chemistry*, **7**, 877 (1996).
 Ichiraku, Y., Stern, S. A. and Nakagawa, T., "An Investigation of the High Gas Permeability of Poly(1-trimethylsilyl-1-propyne)", *J. Membrane Sci.*, **34**, 5 (1987).
 Jacobson, S. H., "Computer Assisted Analysis of X-Ray Scattering for Polymeric Gas Separation and Barrier Materials", *Polym. Prepr.*, **32**, 39 (1991).
 Kesting, R. E. and Fritsche, A. K., "Theory of Gas Transport in Membranes", in "Polymeric Gas Separation Membranes", John Wiley & Sons, New York, NY, 19 (1993).
 Kim, H. J. and Hong, S. I., "The Sorption and Permeation of CO_2 and CH_4 for Dimethylated Polysulfone Membrane", *KJChE*, **14**(3), 168 (1997).
 Kim, T. H., Koros, W. J., Husk, G. R. and O'Brien, K. C., "Relationship between Gas Separation Properties and Chemical Structure in a Series of Aromatic Polyimides", *J. Membrane Sci.*, **37**, 45 (1988).
 Koros, W. J. and Chern, R. T., "Separation of Gaseous Mixtures Using Polymer Membranes", in Rousseau, R. W. (Ed.), "Handbook of Separation Process", Wiley-Interscience, New York, NY, 862 (1987).
 Koros, W. J. and Fleming, G. K., "Membrane-Based Gas Separation", *J. Membrane Sci.*, **83**, 1 (1993).
 McHattie, J. S., Koros, W. J. and Paul, D. R., "Effect of Isopropylidene Replacement on Gas Transport Properties of Polycarbonates", *J. Polym. Sci., Part B, Polym. Phys. Ed.*, **29**, 731 (1991a).
 McHattie, J. S., Koros, W. J. and Paul, D. R., "Gas Transport Properties of Polysulphones: 1. Role of Symmetry of Methyl Group Placement on Bisphenol Rings", *Polymer*, **32**, 840 (1991b).
 McHattie, J. S., Koros, W. J. and Paul, D. R., "Gas Transport Properties of Polysulphones: 2. Effect of Bisphenol Connector Groups", *Polymer*, **32**, 2618 (1991c).
 McHattie, J. S., Koros, W. J. and Paul, D. R., "Gas Transport Properties of Polysulphones: 3. Comparison of Tetramethyl-Substituted Bisphenols", *Polymer*, **33**, 1701 (1992).
 Mulder, M., "Materials and Material Properties", in "Basic Principles of Membrane Technology", Kluwer Academic Publishers, Dordrecht, The Netherlands, 17 (1991).
 Muruganandam, N., Koros, W. J. and Paul, D. R., "Gas Sorption and Transport in Substituted Polycarbonates", *J. Polym. Sci., Part B, Polym. Phys. Ed.*, **25**, 1999 (1987).
 Paul, D. R. and Koros, W. J., "Effect of Partially Immobilizing Sorption and Permeability on the Diffusion Time Lag", *J. Polym. Sci., Part B, Polym. Phys. Ed.*, **14**, 675 (1976).
 Pixton, M. R. and Paul, D. R., "Gas Transport Properties of

- Adamantane-Based Polysulfones", *Polymer*, **36**, 3165 (1995).
- Rautenbach, R. and Welsch, K., "Treatment of Landfill Gas by Gas-Permeation-Pilot Plant Results and Comparison to Alternatives", *J. Membrane Sci.*, **87**, 107 (1994).
- Stern, S. A., "Polymers for Gas Separations: The Next Decade", *J. Membrane. Sci.*, **94**, 1 (1994).
- Van Krevelen, D. W., "Volumetric Properties", in "Properties of Polymers", Elsevier, Amsterdam, The Netherlands, 71 (1990).
- Vieth, W. R., Tam, P. M. and Michaels, A. S., "Dual Sorption Mechanisms in Glassy Polystyrenes", *J. Colloid Interface Sci.*, **22**, 360 (1966).